SOLUTION MINING RESEARCH INSTITUTE

105 Apple Valley Circle
Clarks Summit, PA 18411, USA

Telephone: +1 570-585-8092
Fax: +1 570-585-8091
www.solutionmining.org

Technical Conference Paper

Thermal Effects in Salt Caverns

Mehdi Karimi-Jafari and **Pierre Bérest**

LMS, Ecole Polytechnique, Palaiseau, France

Benoît Brouard

Brouard Consulting, Paris, France

Spring 2007 Conference
29 April -2 May 2007
Basel, Switzerland

Solution Mining Research Institute, Spring 2007 Technical Meeting
Basel, Switzerland, 29 April – 2 May, 2007

THERMAL EFFECTS IN SALT CAVERNS

Mehdi Karimi-Jafari[1], Pierre Bérest[1], Benoît Brouard[2]

[1] LMS, Ecole Polytechnique, Palaiseau, France

[2] Brouard Consulting, Paris, France

ABSTRACT

The temperature of rock increases with depth. However, caverns most often are leached out using soft water pumped from rivers, lakes or shallow aquifers with colder temperature, and the temperature of cavern brine is significantly lower than rock temperature. The difference slowly resorbs with time, due to heat conduction in the rock mass and heat convection in the cavern. This effect has important consequences, especially when the cavern is closed, as brine warming results in pressure build-up in the cavern. Several papers presented during various SMRI Meetings have addressed this problem.

This paper focuses on the following points.

- Influence of cavern shape on temperature increase rate — The increase rate is the slowest in a spherical cavern. Various shapes and sizes are considered, and the brine-warming rate is discussed as a function of cavern shape.
- Convection in the cavern — Due to the geothermal gradient, warmer brine at the bottom of a cavern is slightly less dense than colder brine at the top of a cavern, and a brine cavern is the seat of perennial convective flow. One or several convective cells develop, stirring cavern brine and making the brine-temperature gradient smaller than the geothermal gradient. The influence of cavern size and shape on the convective flow rate is discussed.
- Rock thermal expansion — The brine temperature increase causes heat transfer from the surrounding rock, rock cooling and rock contraction. However, it is proven that rock contraction generates a small, or no, cavern volume change when the cavern shape is cylindrical or spherical.

Keywords: Convection, Thermal Expansion, Brine Warming

1. BRINE WARMING, CHARACTERISTIC TIME

When cold brine or cold water is injected in a cavern (during cavern creation, for example, or before storage cavern abandonment), a significant temperature difference develops between the rock mass, whose virgin temperature is geothermal, and the cavern brine: the rock temperature decreases in the vicinity of the cavern, heat is transferred to the cavern, and brine temperature slowly increases. After a long period of time, the brine temperature equals the geothermal rock temperature. The equations that describe this phenomenon are discussed in Van Sambeek et al. (2005).

From a practical perspective, it is important to assess how fast cavern brine warms up. In fact, the brine-temperature increase rate is a function of both cavern size and cavern shape. For a *spherical* cavern, it has been proven that the time after which 75% of the initial temperature gap is resorbed can be written as

$$t_c = V_c^{2/3} / 4k_{salt}^{th} \quad \text{or} \quad t_c \text{ (years)} \approx V_c \text{ (m}^3\text{)}^{2/3} / 400 \tag{1}$$

where t_c is the "characteristic time", as defined above,

V_c is the cavern volume, and

k_{salt}^{th} is salt thermal diffusivity ($k_{salt}^{th} = 100$ m^2/year is typical).

For example, when $V_c = 8{,}000$ m^3, $V_c^{2/3} \approx 400$ m^2, and the characteristic time is 1 year. Figure 1 illustrates this. Temperature was measured periodically in this 8,000-m^3 cavern, and 75% of the initial temperature difference (which was 45 – 26.5 = 18.5 °C) was resorbed after approximately 1 year.

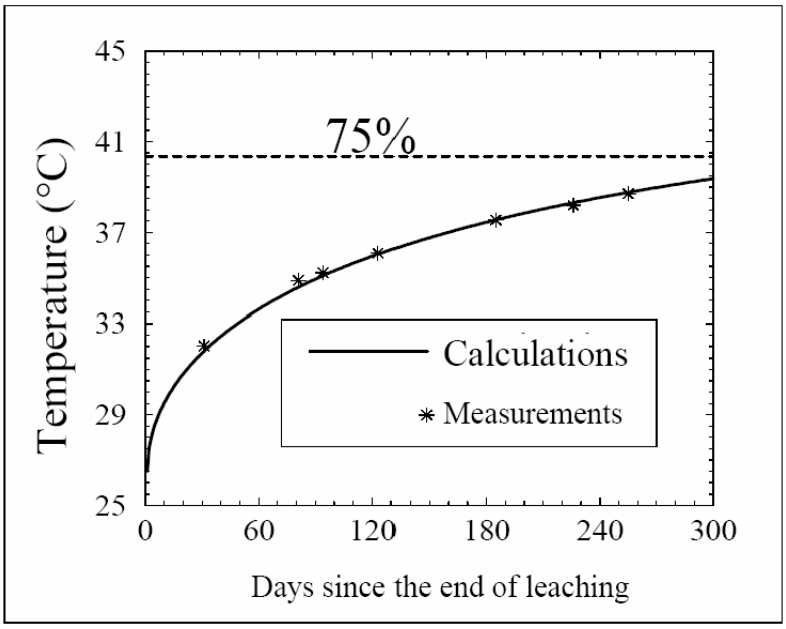

Figure 1 - Brine temperature increase in a 950-m deep, $V_c = 8{,}000$ m^3 brine-filled cavern. Numerical computations fit actual temperature measurements.

This simple former formula holds for a *spherical* cavern. The spherical shape is the less favourable case, in that heat transfer toward a spherical cavern is slower than it is toward any other type of cavern (because the ratio of volume to contour area is largest in a sphere).

In the case of a *cylindrical* cavern, the characteristic time is smaller, the heat transfer rate to the cavern is faster, and thermal equilibrium is reached after a shorter period of time. Numerical computations were performed to assess the characteristic time of cylindrical caverns. The cavern aspect ratio, or $A = H/D$, is the ratio between cavern height (H) and cavern diameter (D). A cavern with $V_c = 100{,}000$ m^3 (600,000 bbls) was considered ($V_c = \pi D^2 H/4$). For a spherical cavern with $V_c = 100{,}000$ m^3, the characteristic time, according to (1), is 5 years. The characteristic time of 100,000 m^3 cylindrical caverns, as a function of cavern aspect ratio, is displayed on Figure 2. It is smaller than the characteristic time of a spherical cavern, even in the case $A = 1$. It is divided by a factor of approximately 2.5 when the cavern is flat ($H/D = 0.1$) or slender ($H/D = 10$).

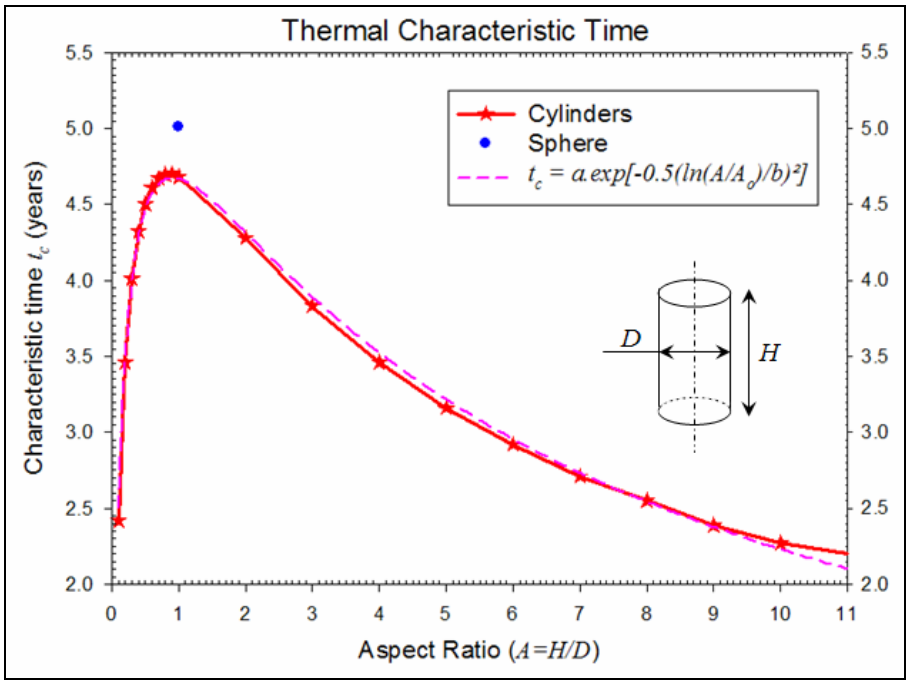

Figure 2 - Heating characteristic time t_c as a function of the aspect ratio for cylindrical caverns ($V = 100{,}000$ m^3).

The following approximation ("normal law") was fitted against numerical computations results in the range $0.1 < A < 10$ using a standard log-normal law:

$$t_c \approx a \cdot \exp\left[-\frac{1}{2}\left(\frac{\ln\left(A/A_o\right)}{b}\right)^2\right] \tag{2}$$

where, $a = 4.67, b = 1.97, A_o = 0.91$ and $V_c = 100{,}000$ m^3.

When a cylindrical cavern with volume $V_c \neq 100{,}000$ m^3 is considered, its characteristic time can be expressed as

$$t_c \approx a \cdot \left[\frac{V_c(m^3)}{100{,}000}\right]^{2/3} \times \exp\left[-\frac{1}{2}\left(\frac{\ln\left(A/A_o\right)}{b}\right)^2\right] \tag{3}$$

where $a = 4.67, b = 1.97$, and $A_o = 0.91$.

2. THERMAL CONVECTION IN A LIQUID-FILLED CAVERN

When heated, most liquids become less dense (an outstanding exception is water in the 0 °C to 4 °C range). For this reason, a liquid at rest is stable only when its temperature is constant in any horizontal plane: temperature must be a function of z only, $T = T(z)$, where z is the Cartesian vertical coordinate, z directed downward. When $dT/dz < 0$ [i.e., when the thermal gradient is directed upward (cold fluid below warm fluid), the liquid at rest is stable. When $dT/dz > 0$ (warm fluid below cold fluid), things are slightly more complicated. When the thermal gradient is positive but small, the fluid can be stable provided that the thermal gradient is smaller than the so-called *adiabatic gradient*, or the change in temperature experienced by a drop of fluid moving upward when the pressure of the fluid drop decreases to stay in mechanical equilibrium with

the surrounding fluid. (This is the reason why hot air sometimes remained trapped at ground level even when the temperature at heights is colder.) The adiabatic gradient in the case of liquids such as water or brine is very small. When $dT/dz > 0$ and dT/dz is large enough, the fluid is unstable. For instance, in a brine-filled cavern, because of the geothermal gradient (which typically is $dT/dz = 0.016\,°\mathrm{C/m}$ in a salt formation), brine at the cavern bottom is warmer than brine at the cavern top. It is also lighter: it moves upward, and cold brine moves downward. This movement is called (brine) "thermal convection". Because the geothermal gradient is perennial, the brine flow in the cavern never stops. It is more intense after a large injection of cold water or brine at the top of the cavern, but, even after a long period of time during which the cavern remains idle, brine thermal convection is active, as it will be still several centuries after cavern abandonment. An example of this is provided on Figure 3.

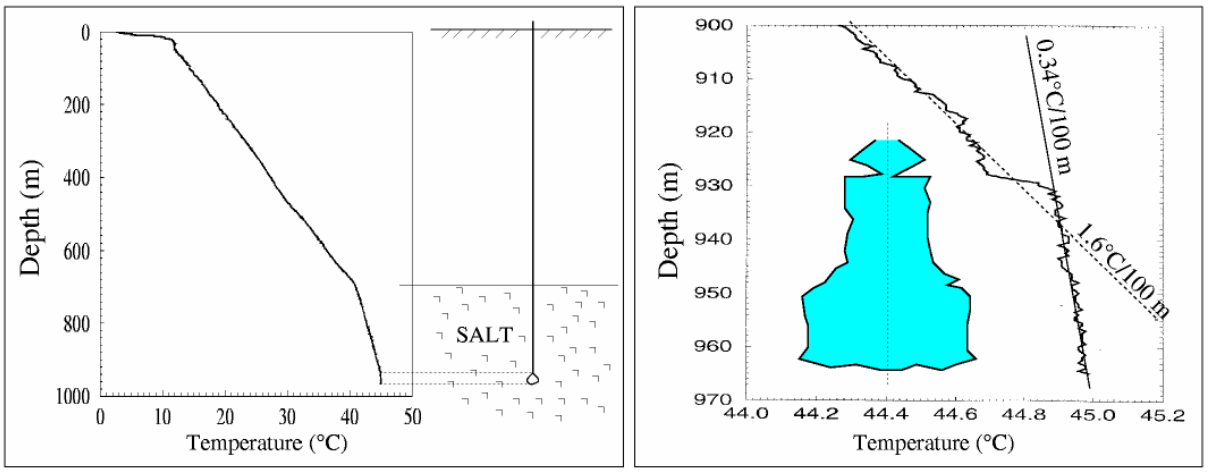

Figure 3 - Well and cavern temperatures in EZ53 well (Etrez, France).

The cavern depicted in Figure 3 had been leached-out by 1982 and remained idle from 1982 to 1996. Temperature equilibrium was met in this 8,000-m^3 cavern after 14 years. (Characteristic time is $t_c \approx 1$ year .) The geothermal gradients in the salt formation (1.6 °C / 100 m) and in the overlying formation of marls can be observed easily. The geothermal gradient in the cavern itself (0.34 °C / 100 m) is quite small, proof of the existence of thermal convection that effectively stirs cavern brine and makes its temperature much more homogeneous than it would be were the brine to remain at rest.

Fluid convection in a cavern often is described, according to the so-called Boussinesq approximation, by the following set of equations:

$$\begin{cases} \mathrm{div}\,\vec{u} = 0 \\ \rho_f \dfrac{d\vec{u}}{dt} = -\overrightarrow{grad}\left(P - \rho_f g z\right) + \mu_f \Delta\vec{u} - \alpha_f \rho_f \theta_f \vec{g} \\ \dfrac{\partial \theta_f}{\partial t} + \left[\left(\dfrac{dT}{dz}\right)_{geothermal} \cdot \vec{e}_z + \overrightarrow{grad}\ \theta_f\right] \cdot \vec{u} = k_f \Delta\theta_f \end{cases} \tag{4}$$

where P is fluid pressure,

ρ_f is fluid density,

$\vec{u}$ is fluid velocity ,

μ_f is fluid dynamic viscosity,

α_f is fluid thermal expansion coefficient,

k_f is fluid thermal diffusivity and

θ_f is the difference between fluid temperature and geothermal temperature at fluid depth.

It is convenient to set $\mathrm{Pr} = \mu_f / \rho_f k_f$ (Prandtl number) and $\mathrm{Gr} = \rho_f{}^2 g \alpha_f R^4 \left(dT/dz\right)_{geothermal} / \mu_f{}^2$ (Grashof number), where R is the characteristic length and $\left(dT/dz\right)_{geothermal}$ is the geothermal gradient.

Table 1 gives typical examples of Prandtl and Grashof numbers in the case of free convection in brine and methane. Considered pressure and temperature are 10 MPa and 30°C respectively.

Table 1 - Prandtl and Grashof number in the case of convection in brine and methane.

Fluid	Pr	Gr
Brine	7.93	4.3×10^{11}
Methane	0.66	1.2×10^{14}

Within the rock mass, the Fourier equation holds:

$$\begin{cases} \dfrac{\partial \theta_R}{\partial t} = k_R \Delta \theta_R \\ K_f \left.\dfrac{\partial \theta_f}{\partial n}\right|_f = K_R \left.\dfrac{\partial \theta_R}{\partial n}\right|_R \quad \text{at cavern wall} \end{cases} \tag{5}$$

where θ_R is the difference between the disturbed temperature of the rock and the geothermal temperature at rock depth,

k_R is the rock thermal diffusivity.

K_f and K_R are fluid and rock thermal conductivities respectively.

This set of equations was solved numerically using Adina CFD code for various cavern shapes. The Grashof number is relatively high, and turbulent flow must be considered; a kε-standard model was selected.

Four different cavern shapes were considered (Table 2 and Figure 4). A zero temperature was set a mesh top; a vertical temperature gradient dT/dz was set on the right boundary. T_R is the relative temperature at cavern average depth. (To get the actual temperature at any depth, the geothermal temperature at mesh top must be added.)

Table 2 - Considered cavern shapes.

Case #	Cavern shape	Radius (m)	Height (m)	$\frac{dT}{dz}$ (°C/m)	T_R (°C)
1	Flat cylindrical cavern	15	6	0.01	0.25
2	Tall cylindrical cavern	5	50	0.01	0.75
3	Spherical cavern	10	20	0.01	0.4
4	Real-shaped cavern	≈ 8	≈ 40	0.016	0.4

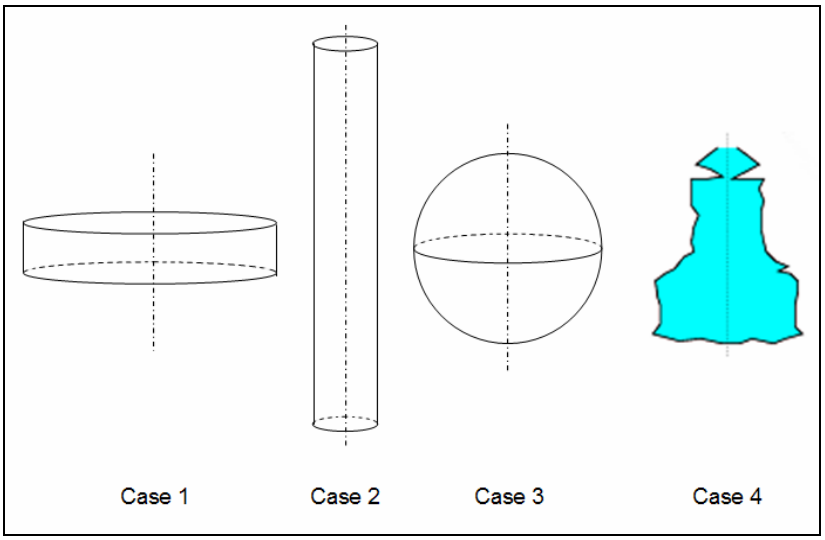

Figure 4 – Considered cavern shapes.

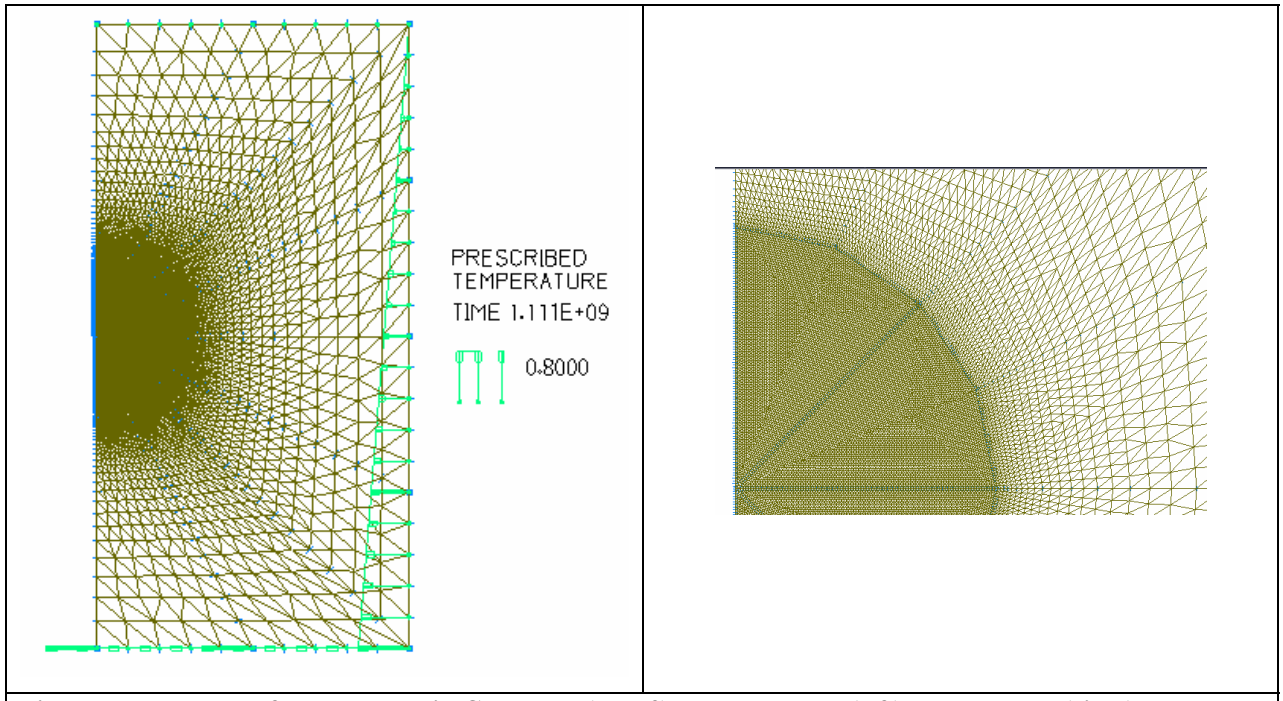

Figure 5 – Example of a mesh used in CFD code (case 3) – Whole mesh (left) and close up (right). There are 43,352 elements and 21,827 nodes.

Case 1 – Flat cylindrical cavern

In this case, a flat cylindrical cavern is considered. The steady-state stream function is given on Figure 6: brine is moving upward on the cavern axis (left part of the figure). The steady-state cavern temperature difference, or θ, and velocity magnitude are given on Figure 7 and Figure 8, respectively. Brine is moving much faster close to cavern axis than in the outer part of the cavern.

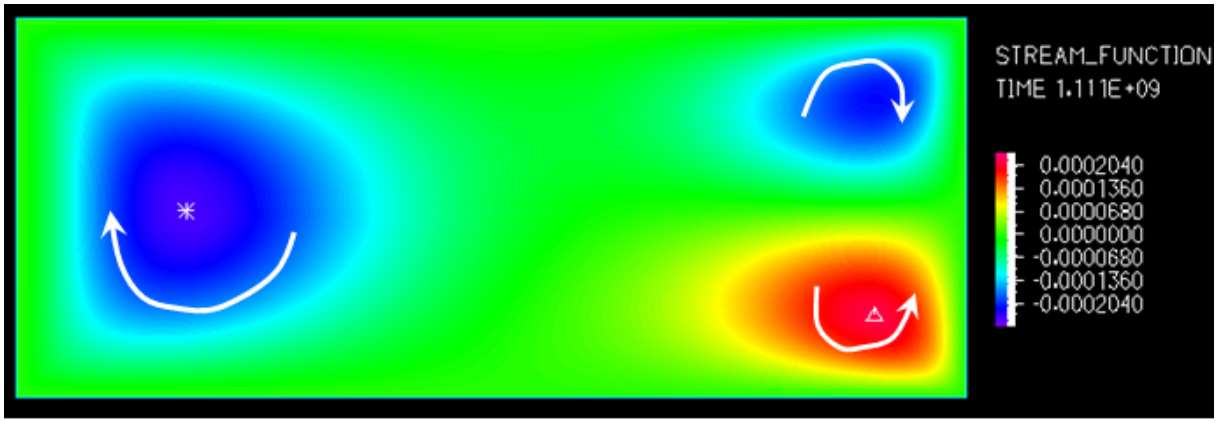

Figure 6 – Case 1, Steady-state stream function in a flat cylindrical cavern.

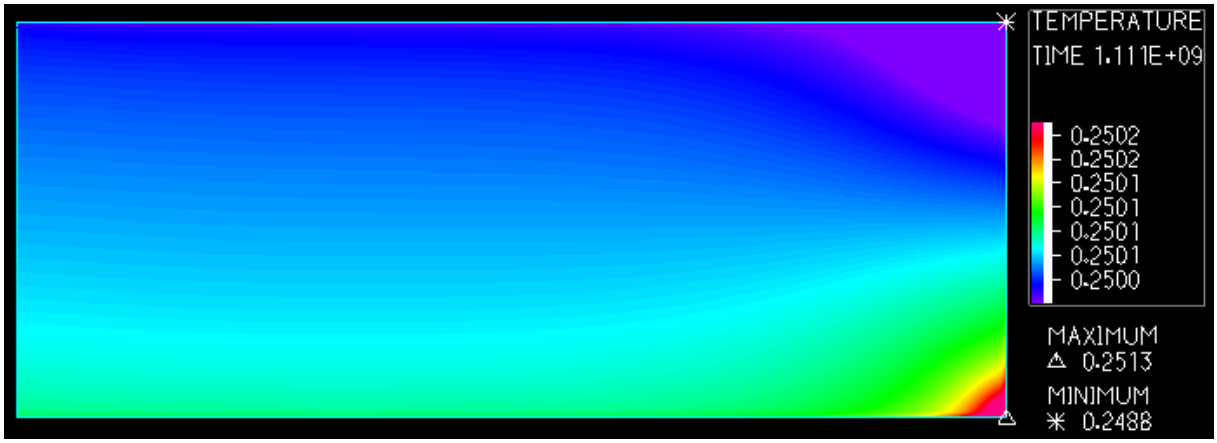

Figure 7 – Case 1, Steady-state temperature (in °C) in a flat cylindrical cavern.

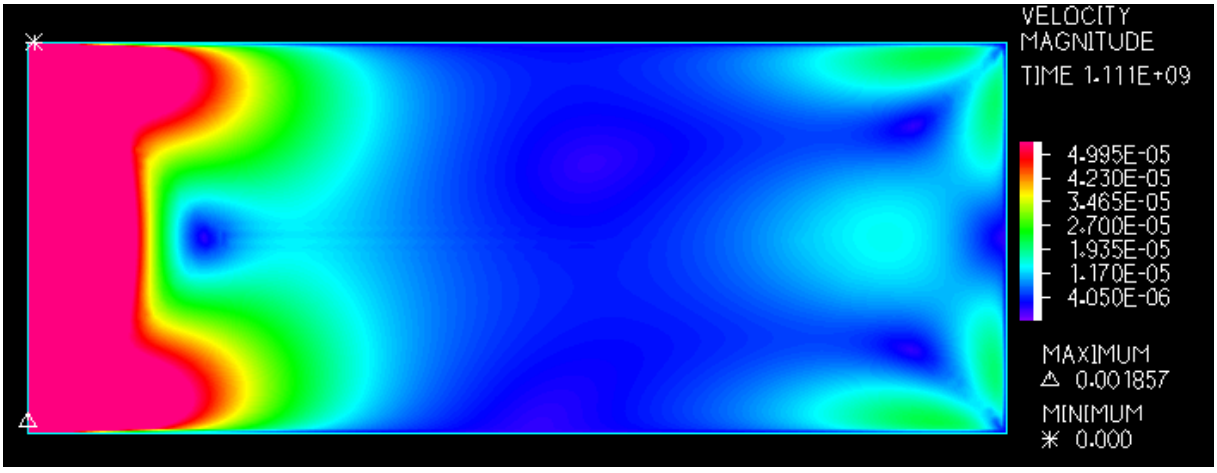

Figure 8 – Case 1, Steady-state velocity magnitude (in m/s) in a flat cylindrical cavern.

Case 2 — Tall cylindrical cavern

In this case, a tall cylindrical cavern is considered. The steady-state stream function, cavern temperature and velocity magnitude are given on Figure 9. Brine is moving upward on the cavern axis.

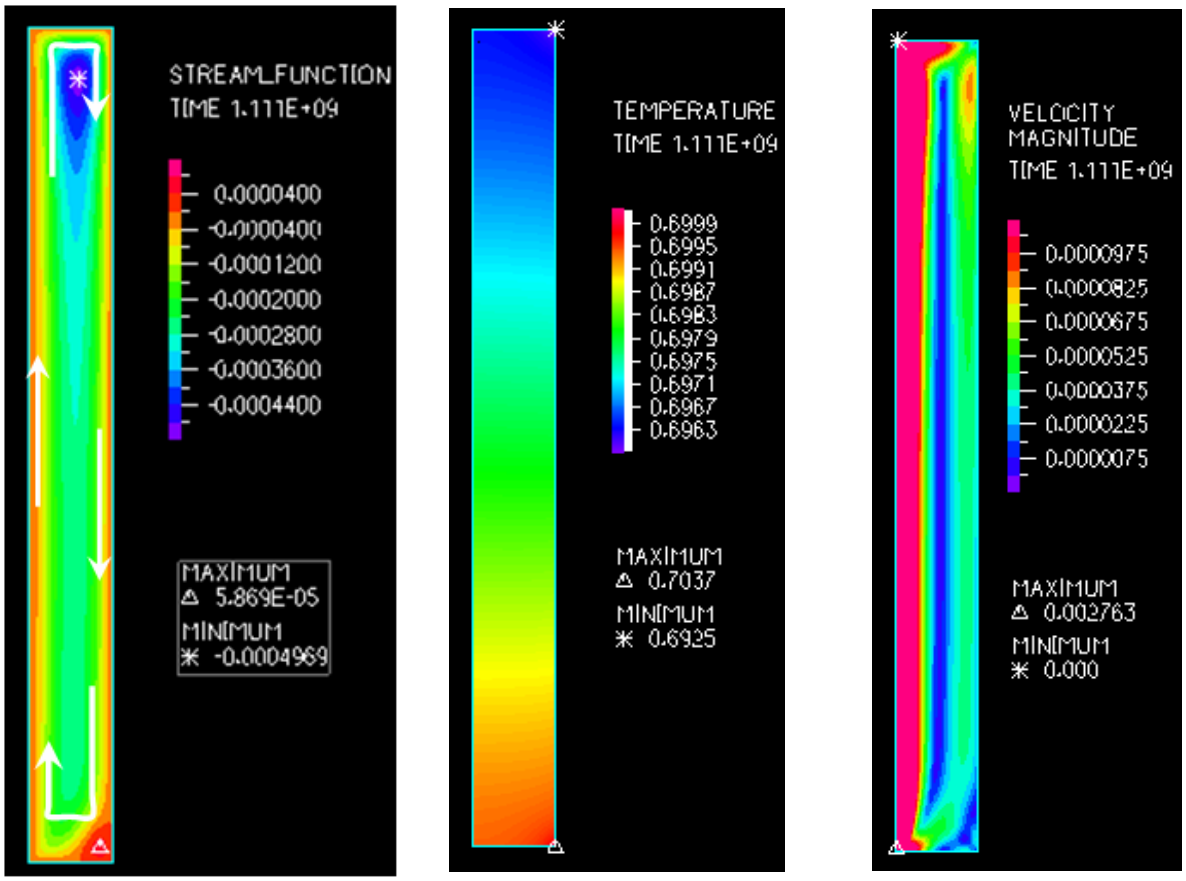

Figure 9 - Case 2, Steady-state stream function (left), temperature (centre), and velocity magnitude (right) in a tall cylindrical cavern.

Case 1— Spherical cavern

A spherical cavern is considered here. The steady-state stream function, cavern temperature and velocity magnitude are given on Figure 10. Brine is moving upward on the cavern axis. There is one large convection cell that is turning clockwise.

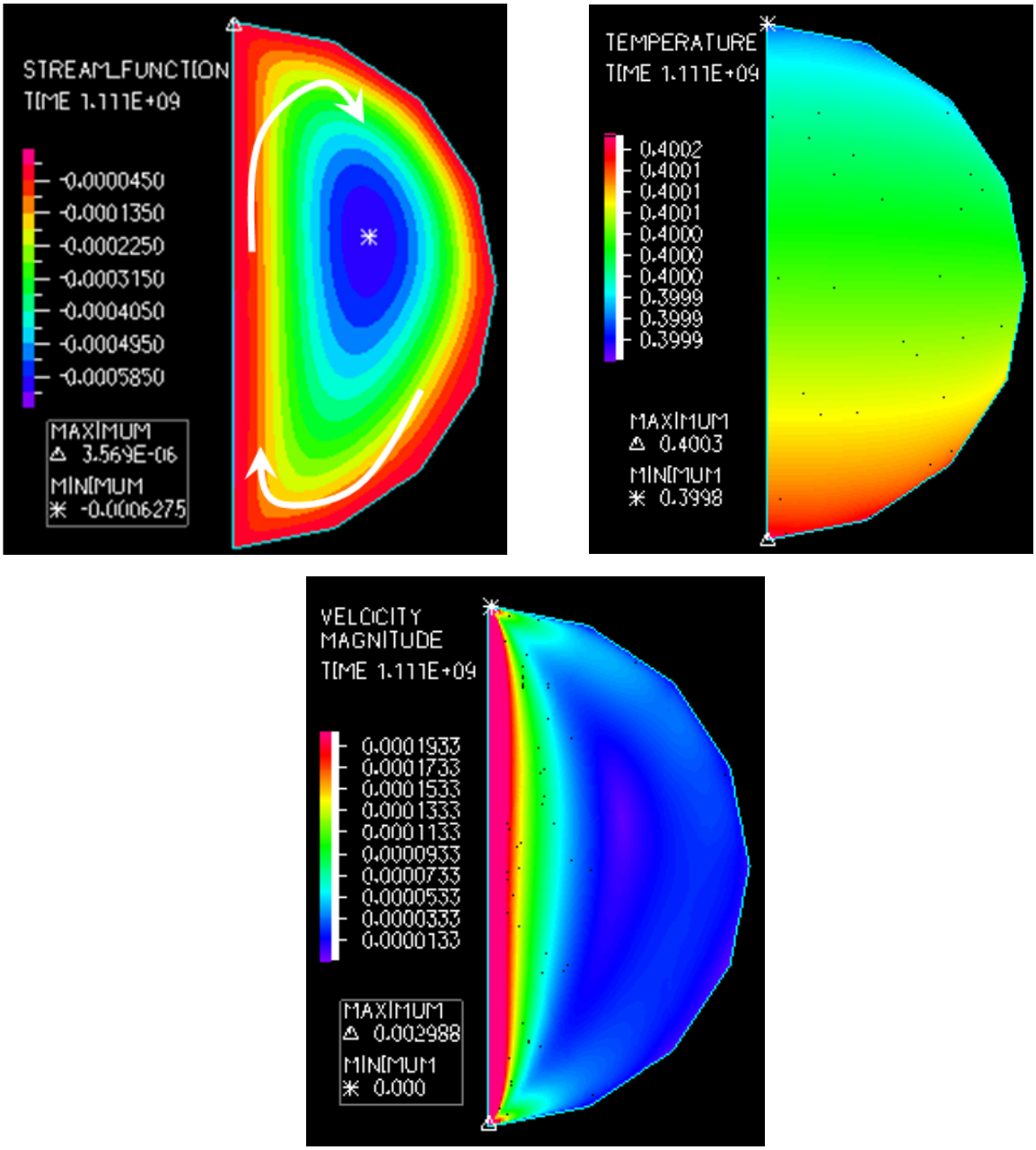

Figure 10 - Case 3, Steady-state stream function (top left), temperature (top right), and velocity magnitude (bottom) in a spherical cavern.

Case 4 – Real-shaped cavern

In this case, a real-shaped cavern is considered; this is EZ53 cavern from Etrez site. Its volume is approximately 8,000 m^3. The steady-state stream function, cavern temperature and velocity magnitude are given on Figure 11. There are three main convection cells. One relatively large cell is turning anticlockwise at cavern bottom.

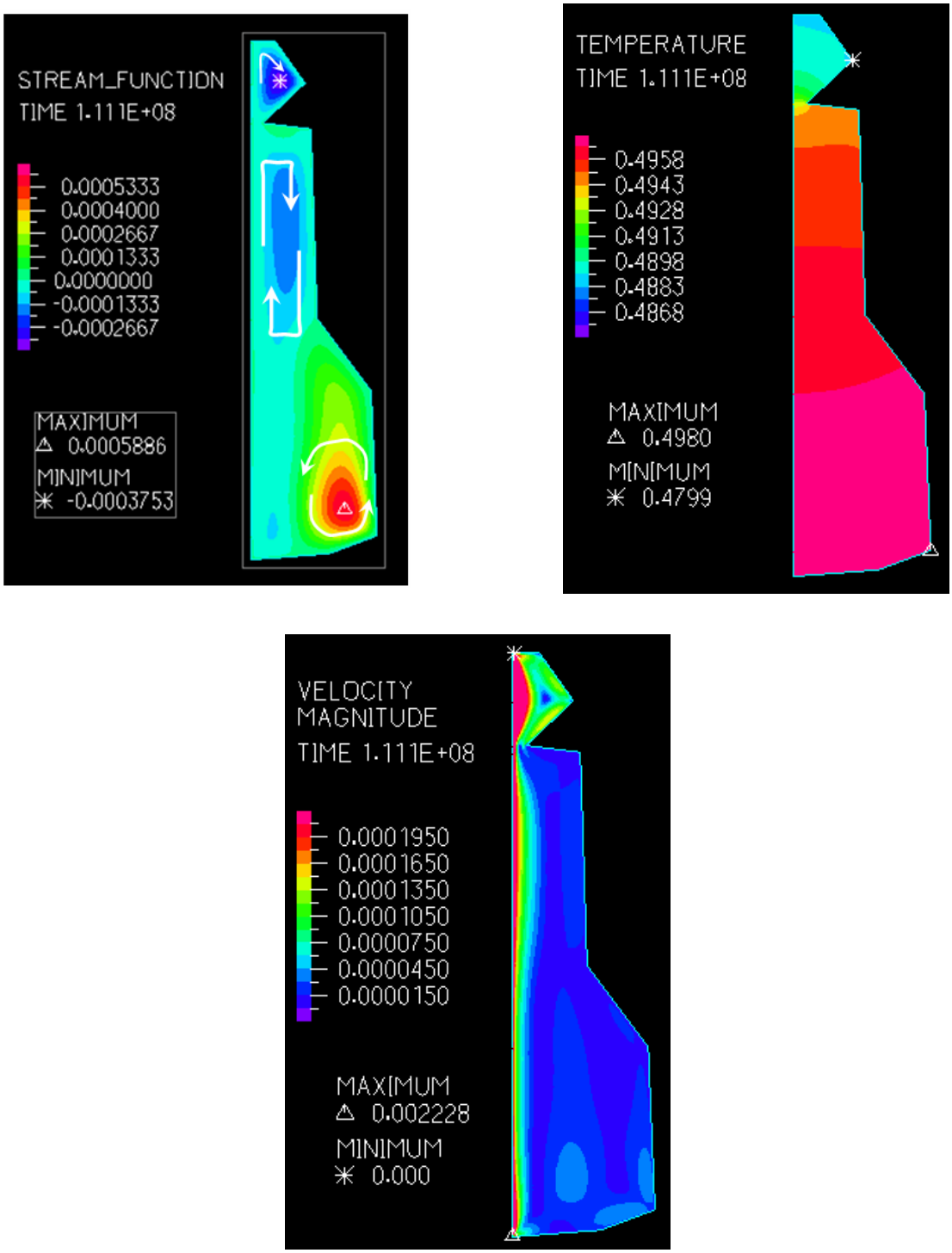

Figure 11 - Case 4, Steady-state stream function (left), temperature (centre), and velocity magnitude (right) in EZ53 cavern (Etrez, France).

3. ROCK MASS THERMAL EXPANSION

When a salt sample is heated uniformly by θ, the following occurs.

- When the sample is allowed to expand freely, the change in sample volume is $\Delta V/V = 3\alpha_R\theta$, where α_R is the rock linear thermal expansion coefficient. ($\alpha_R \approx 4\times10^{-5}$ /°C is typical).

- When the sample is set in a perfectly rigid box, the sample mean stress increases by $\Delta\sigma = E\alpha_R\theta$.

When a fluid-filled cavern is created in a rock mass, any brine temperature change results in heat transfer to or from the rock mass. The rock in the vicinity of the cavern experiences temperature change and thermal expansion or contraction, and the cavern volume may change. It is important to assess the cavern volume change. For example, in a closed cavern, the cavern volume change will generate pressure build-up or pressure decrease. In fact, it has been proven (see the Appendix) that, in the case of an idealized perfectly spherical (or cylindrical), **temperature changes in the cavern rock mass generate no change in the cavern volume**. Numerical computations were performed for an axisymmetric cavern shape — neither spherical nor cylindrical. It was proven that the cavern volume change due to changes in rock temperature is exceedingly small.

APPENDIX

Consider an infinite homogeneous, isotropic, linear elastic medium in which a cavern is created. Two problems can be discussed.

1. The rock mass temperature is unchanged, and a pressure, P, is applied at the cavern wall. The following equations hold:

$$\varepsilon^1_{ij} = L_{ijkl}\sigma^1_{kl} \text{ in the rock mass ; } \sigma^1_{kl}n_l = -Pn_k \text{ at cavern wall}$$

2. The rock mass temperature is changed by $\theta = \theta(x,y,z)$ and no pressure is applied at the cavern wall. The following relations hold:

$$\varepsilon^2_{ij} = L_{ijkl}\sigma^2_{kl} + \alpha_R\theta\delta_{ij} \text{ in the rock mass ; } \sigma^2_{kl}n_l = 0 \text{ at cavern wall}$$

Multiplying the second relation by σ^1_{ij} and subtracting it from the first relation multiplied by σ^2_{ij} leads to a scalar relation that can be integrated over the entire rock mass (Maxwell-Betti); integration per part leads to:

$$\int_{\text{wall}} Pu^1_i n_i da = \iiint_{\text{rock mass}} \alpha_R\theta\sigma^1_{ii} d\Omega$$

In the case of a cylindrical or spherical cavern, it is known that $\sigma^1_{ii} = 0$ and that the cavern volume change is zero:

$$\Delta V_c/V_c = -\int_{\text{wall}} u^1_i n_i da = 0$$

REFERENCES

Bannach A., Wagler T., Walden S. Klafki M., Köckritz V., Mulkamanov A., and Kneer A. *Technology enhancements for (1) inventory assessment and mechanical integrity testing of gas-filled solution mined caverns and (2) mechanical integrity tests of solution mining and liquid storage caverns*. Report prepared for the Gas Research Institute, Ref. GRI-05/0175, 73 pages (2005).

Markatos N. C. and Pericleous K. A. *Laminar and turbulent natural convection in an enclosed cavity*. Int. J. Heat Mass Transfer, Vol.27, No.5, pp.755-772 (1984).

Van Sambeek L.L., Bérest P., and Brouard B. *Improvements in Mechanical Integrity Tests for solution-mined caverns used for mineral production or liquid-product storage*. SMRI Research Project Report. 142 pages (2005).